# Ordinary Differential Equations in Green Oxidation Processes

Angela Dapolite
Department of Chemical Engineering
Clarkson University

**Project Mentor**
Maria Emelianenko

## Abstract

This paper explores the numerical and analytical techniques that can be used to solve a 3D system of nonlinear ordinary differential equations that describe the oxidation of a Safranine dye. One goal of this project is to find the set of reaction rate constants that fit experimental data for all initial conditions. A least squares fitting, using ode23s from matlab, was used to obtain rate constant values for the reaction rates $k_2$ and $k_3$. An exact solution to this 3D nonlinear system could not be obtained from the equations as is. It was found that this specific system can be transformed from a 3D system to a 2D system; linearizing the 2D system led to a set of analytical equations that represented the solution to the 2D system. The analytical solution for the concentration of the dye was compared to the experimental data at the $k_2$ and $k_3$ values obtained from the numerical fitting. For different initial conditions, it was found that different pairs of $k_2$ and $k_3$ values were obtained.

# 1   Introduction

Oxidation, a process in which oxygen is added to break pollutants or organic wastes, is important in many industries. However, this process often uses chemicals that can result in the production of hazardous substances [1]. Because oxidation is an important process, it is imperative that oxidation occurs in a manner that is environmentally safe.

Researchers in the Chemistry Department at Carnegie Mellon University in Pittsburgh, Pennsylvania have proposed that the use of hydrogen peroxide to aid in oxidation is environmentally safe. They have developed catalysts, substances which help chemical reactions occur, known as tetraamidomacrocyclic-ligand, or TAML, activators; in particular, Fe-TAML activators have been developed. These activators work in conjunction with hydrogen peroxide to activate chemical reactions to occur. During this process, known as green chemistry, harmful pollutants are converted to less toxic substances [1].

These Fe-TAML activators can be applied to many areas of research; one such area of interest has been the pulp and paper industry. Researchers at Carnegie Mellon University have speculated that toxic compounds and colored pollutants resulting from paper and wood pulp processing can be destroyed using Fe-TAML activators. Typically, to make paper white, the pulp and paper industry has used chlorine dioxide to activate oxidation that leads to bleaching. However, bleaches that contain chlorine compounds have been known to contaminate the water supply. Thus, an alternate, environmentally safe method is to use the TAML activators combined with the hydrogen peroxide solution. These catalysts have been shown to improve pulp bleaching and do not contaminate the water supply [1].

In general, Fe-TAML activators can be used for the oxidation of many organic targets, including environmental pollutants, drugs, and dyes by the use of hydrogen peroxide.

# 2 Project Description

## 2.1 Background

This project is a joint effort with Dr. Ryabov's Chemistry group at Carnegie Mellon University; it explores the Fe-containing catalysts for the oxidation of a Safranine dye.

For this project, a new ligand system introduced is the D generation of TAMLs, and it is an innovative step towards the development of man-made oxidizing catalysts for various environmental tasks. As compared to the Fe-TAML catalysts of the previous B generation, the D family should have significant advantages including the following:

(i) synthetic affordability and accessibility of the D TAML ligand system,

(ii) the hydrolytic stability of FeIII-TAML complexes,

(iii) the operational stability of FeIII-TAML complexes,

(iv) higher catalytic activity in terms of the speed of activation of a primary oxidant ($k_1$) and the speed of oxidation of a target electron donor ($k_2$), and

(v) the closest to neutral pH optimum of the highest catalytic activity [2].

This new catalyst has been predicted to help solve various problems facing humanity; it can aid in water purification, destroying pesticides, and disinfection.

## 2.2 Problem Statement

The following set of differential equations describe the chemical reactions for the above ligand D system:

$$\frac{dx}{dt} = -k_1^* x + k_2 yz \tag{1}$$

$$\frac{dy}{dt} = k_1^* x - k_2 yz - k_3 y \tag{2}$$

$$\frac{dz}{dt} = -k_2 yz \tag{3}$$

where $k_1^* = k_1 * [H_2O_2]$.

In these differential equations, x represents the concentration of the resting catalyst Fe-TAML, y represents the concentration of the active catalyst, and z represents the concentration of the Safranine dye; $k_1, k_2$ and $k_3$ are all positive rate constants.

Equation (1), above, shows that the resting catalyst disappears when it reacts with the hydrogen peroxide; it then reappears when the resting catalyst reacts with the dye. Equation (2) depicts that the active catalyst is produced when the resting catalyst reacts with hydrogen peroxide, and disappears when it reacts with the dye; furthermore, the active catalyst proceeds to kill itself, as represented by the third term. Equation (3) conveys that bleaching of the dye occurs when the dye reacts with the active catalyst.

The main goal of this project is to understand the system as thoroughly as possible from both an analytical and numerical perspective. Specifically, it is of interest to predict the optimal values for the rate constants $k_2$ and $k_3$ by using

3

experimental data provided by Carnegie Mellon chemists; one goal is to see if a set of k values, $k_1$, $k_2$, and $k_3$ exists such that they fit all experimental data for all initial conditions. To assist in this, the chemists have provided the value of $k_1$, the initial concentrations of x, y, and z, the concentration of $[H_2O_2]$ and the concentration profile of z at various instances in time.

# 3    Research Methods

To understand the system of equations, both an analytical approach and a numerical approach were used.

## 3.1    Analytical Approach

### 3.1.1    Stability Analysis

Because this system is a 3-D nonlinear system, an exact solution cannot be directly obtained. To better understand the system, I found the critical points and respective eigenvalues to classify the stability. To find the critical points, I set equations (1), (2), and (3) equal to zero and solved the resulting system. For this system, I found that there were two critical points. These two points are (0,0,0) and $(0,0,\frac{k_3}{k_2})$. Once each critical point was found, I set up the Jacobian matrix at each critical point. At (0,0,0), the Jacobian matrix is shown below:

$$\begin{pmatrix} -k_1^* & 0 & 0 \\ k_1^* & -k_3 & 0 \\ 0 & 0 & 0 \end{pmatrix}$$

From this matrix, eigenvalues were calculated to determine the stabililty of the system at (0,0,0). The calculated eigenvalues are $\lambda_1 = 0$, $\lambda_2 = -k_1^*$, and

4

$\lambda_3 = -k_3$. This information tells us that at (0,0,0) there is a degenerate stable node, since one of the eigenvalues is zero and the other two are negative.

At $(0,0,\dfrac{k_3}{k_2})$, the Jacobian matrix is displayed below:

$$
\begin{pmatrix}
-k_1^* & k_3 & 0 \\
k_1^* & -2k_3 & 0 \\
0 & -k_3 & 0
\end{pmatrix}
$$

From this matrix, the caculated eigenvalues are $\lambda_1 = 0$,
$\lambda_2 = \dfrac{k_1^* + 2k_3}{-2} + \dfrac{\sqrt{(k_1^*)^2 - 8k_1^* k_3 + 4k_3^2}}{-2}$, and $\lambda_3 = \dfrac{k_1^* + 2k_3}{-2} - \dfrac{\sqrt{(k_1^*)^2 - 8k_1^* k_3 + 4k_3^2}}{-2}$.
This information tells us that at $(0,0,\dfrac{k_3}{k_2})$ there are two situations; if the discriminent $(k_1^*)^2 - 8k_1^* k_3 + 4k_3^2$ is negative, then there are two complex roots, leading to a degenerate spiral. If $(k_1^*)^2 - 8k_1^* k_3 + 4k_3^2$ is positive, then a degenerate stable node exists.

### 3.1.2   Transformation to a Lienard System

One possible path towards an analytical solution is to transform the 3D system into a 2D system. Since t is the only independent variable in the system, $\dfrac{dx}{dt}, \dfrac{dy}{dt}$, and $\dfrac{dz}{dt}$ will be denoted by $x', y'$, and $z'$ respectively.

Adding equations (1) and (2) tells us that

$$x' + y' = -k_3 y \tag{4}$$

Furthermore equation (3) yields that

$$(\log(z))' = -k_2 y \tag{5}$$

Together, equations (4) and (5) imply that

$$(\log(z))' = \frac{k_2}{k_3}(x+y)' \tag{6}$$

Integrating equation (6) yields

$$\log(z) = \frac{k_2}{k_3}(x+y) + C^* \tag{7}$$

where $C^*$ is a constant of integration. Exponentiating (7) results in the following equation for z:

$$z = Ce^{\frac{k_2}{k_3}(x+y)} \tag{8}$$

for some constant C. Also, equation (4) implies that

$$x = -k_3 \int y - y + C' \tag{9}$$

Plugging x from (9) into (8) yields

$$z = Ce^{-k_2(\int y)} \tag{10}$$

Introducing a new variable $v$,

$$v \equiv \int y,$$

6

we get that (1) turns into a second order non-linear homogeneous equation described by the following:

$$v'' = k_1(-k_3 v - v') - k_2 C v' e^{-k_2 v} - k_3 v' \tag{11}$$

Or,

$$v'' + (k_1 + k_3 + C k_2 e^{-k_2 v})v' + k_1 k_3 v = 0 \tag{12}$$

This system is of the form $v'' + f(v)v' + g(v) = 0$, which belongs to the family of Lienard systems [3] with $f(v) = k_1 + k_3 + C k_2 e^{-k_2 v}$ and $g(v) = k_1 k_3 v$.

This Lienard system can be written in an equivalent form as

$$v' = u \tag{13}$$

$$u' = -g(v) - f(v)u \tag{14}$$

Thus, the 3D system has now been transformed into a 2D system.

Doing a stability analysis of this 2D system yields one critical point at (0,0) with eigenvalues $\lambda_1 = \dfrac{-k_1^* - k_3 - C k_2}{2} + \dfrac{\sqrt{(k_1^*)^2 + 2C k_1^* k_2 + 2C k_2 k_3 + k_3^2 + C^2 (k_2)^2 - 2k_1^* k_3}}{2}$ and $\lambda_2 = \dfrac{-k_1^* - k_3 - C k_2}{2} - \dfrac{\sqrt{(k_1^*)^2 + 2C k_1^* k_2 + 2C k_2 k_3 + k_3^2 + C^2 (k_2)^2 - 2k_1^* k_3}}{2}$;
a closer look at these eigenvalues suggests that there is a stable node at this critical point.

From numerical results, in each case $k_2$ is large, on the order of $10^3$. Our numerical data shows that $k_1^*$ is 5, and $k_3$ is on the order of $10^{-3}$. When these values are plugged into (14) for f(v), the exponential term approaches zero; thus, the lienard system can be reduced to the following set of linear differential

7

equations:

$$v' = u \tag{15}$$

$$u' = -k_1^* k_3 v - (k_1^* + k_3)u \tag{16}$$

This system can now be solved analytically by finding the eigenvalues and resulting eigenvectors; the solution follows below:

$$v = C_1 e^{-k_1^* t} + C_2 e^{-k_3 t} \tag{17}$$

$$u = -k_1^* C_1 e^{-k_1^* t} - k_3 C_2 e^{-k_3 t} \tag{18}$$

Using these transformed variables, an analytical solution for x, y, and z can be rewritten as

$$x = -k_3 (C_1 e^{-k_1^* t} + C_2 e^{-k_3 t}) + k_1^* C_1 e^{-k_1^* t} + k_3 C_2 e^{-k_3 t} \tag{19}$$

$$y = -k_1^* C_1 e^{-k_1^* t} - k_3 C_2 e^{-k_3 t} \tag{20}$$

$$z = C e^{-k_2 (C_1 e^{-k_1^* t} + C_2 e^{-k_3 t})} \tag{21}$$

In each of these equations, it is imperative to find the values of $C$, $C_1$, and $C_2$. Algebraic manipulation yields the following results for these constants.

$$C = z(0) e^{k_2 (C_1 + C_2)} \tag{22}$$

$$C_1 = \frac{x(0)}{(k_1^* - k_3)} \tag{23}$$

$$C_2 = \frac{y(0)}{k_1^* - k_3} - \frac{k_1^* (x(0) + y(0))}{k_3 (k_1^* - k_3)} \tag{24}$$

Using the $k_1^*$ value provided, the initial values for x, y, and z, and the $k_2$ and $k_3$ rate constants found by the numerical optimization, the constants $C$, $C_1$,

8

and $C_2$ can be calculated. Using (21), concentrations for z were found. The analytical solution for z was then graphed with the experimental data to see how well the analytical solution fit the data.

One last analytical technique was to solve for $k_2$. Using equations (10), (17), and (22), the following equation for z is obtained

$$z = z(0)e^{k_2(C_1 + C_2 - C_1 e^{-k_1^* t} + C_2 e^{-k_3 t})} \qquad (25)$$

Taking the logarithms of both sides and solving for $k_2$ yields the following equation

$$k_2 = \frac{\log(z) - \log(z(0))}{C_1 + C_2 - C_1 e^{-k_1^* t} - C_2 e^{-k_3 t}} \qquad (26)$$

Using the $k_1^*$ value provided, the expressions for $C_1$ and $C_2$, the value obtained for $k_3$ from the numerical solution, and time and z concentrations from the data set, $k_2$ can be obtained from equation (26). These $k_2$ values were then compared with the $k_2$ values from the numerical solution.

## 3.2 Numerical Approach

### 3.2.1 Least Squares Fitting

Numerical techniques can also be used to solve the differential equations as depicted in (1), (2), and (3). In matlab, a least squares fitting was applied to minimize the error between the experimental data and the numerical curve. Ode 23s was used because we had a stiff system; by a stiff system, this means that the values of the rate constants differed significantly. By setting the value of $k_1^*$ to 5, and by setting an initial range of $k_2$ and $k_3$ values to search at, $k_2$ and $k_3$ parameter values were obtained using ode23s and fminsearch; this occurred when the difference between the experimental and numerical curves was

minimized. An error value was outputted, and graphs were obtained to visually see the fit between the numerical curve and experimental data at the $k_2$ and $k_3$ values.

Using the values obtained for the constants $C$, $C_1$, and $C_2$, as well as the initial conditions and experimental data, a function call fmincon in matlab was used to find the rate constants $k_2$ and $k_3$; fmincon was used to ensure that $k_2$ and $k_3$ were both nonnegative. These values were compared with the parameter values obtained using fminsearch. Graphs were also produced to see how the analytical solution for z at these reaction rate values fit the experimental data.

# 4    Results and Discussion

The chemists at Carnegie Mellon University provided data showing the bleaching of the Safranine dye by hydrogen peroxide at various instances in time. For each set of data, $x(0) = 2.18 \times 10^{-7}$ and $y(0) = 0$, and the value for $z(0)$ varies between each set; the value of $k_1^*$ was also provided and set at 5.

Using this information, a least squares fitting analysis was done using ode23s and fminsearch to predict the optimal values of $k_2$ and $k_3$. The table below shows these results at different initial values for z.

| $z(0)$ | $4.63 \times 10^{-5}$ | $3.66 \times 10^{-5}$ | $2.72 \times 10^{-5}$ | $1.72 \times 10^{-5}$ | $6.53 \times 10^{-6}$ |
|---|---|---|---|---|---|
| $k_2$ | $3.3373 \times 10^3$ | $5.0992 \times 10^3$ | $5.0836 \times 10^3$ | $6.3992 \times 10^3$ | $1.1828 \times 10^4$ |
| $k_3$ | $2.6001 \times 10^{-3}$ | $3.3212 \times 10^{-3}$ | $3.0784 \times 10^{-3}$ | $3.2515 \times 10^{-3}$ | $3.5192 \times 10^{-3}$ |

Table 1: Optimal values of $k_2$ and $k_3$ from least squares fitting with ode23s and fminsearch

These optimal values were plugged back into equations (1), (2), and (3), and

10

compared with the experimental data, which is displayed in the figure below.



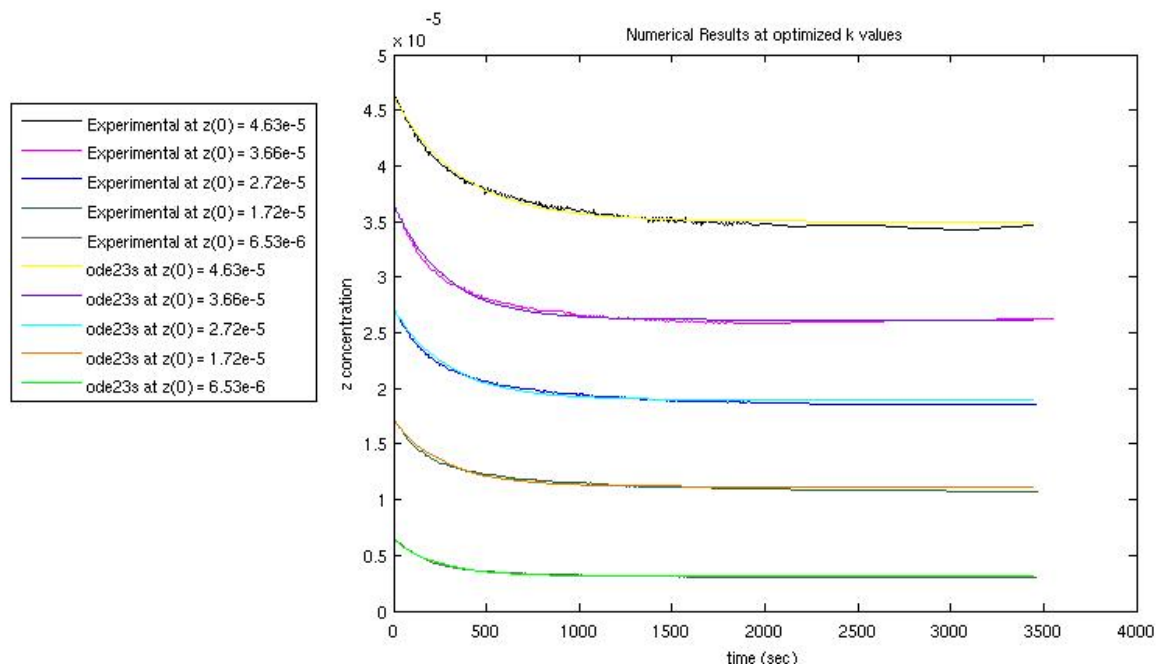Figure 1: Graph of numerical solution and experimental data with rate constant values from least squares fitting

As shown in Table 1, the values for $k_2$ and $k_3$ vary with different initial values for z. Figure 1 shows the fit between the experimental data and the numerical solution at these optimal rate constant values. As can be seen by this graph, these parameters fit the data well, thus conveying that different k values fit different sets of data.

A graph was also produced using the rate constant values in Table 1 to see how well the analytical solution in equation (21) fit the experimental data. The graph is pictured in Figure 2, below.
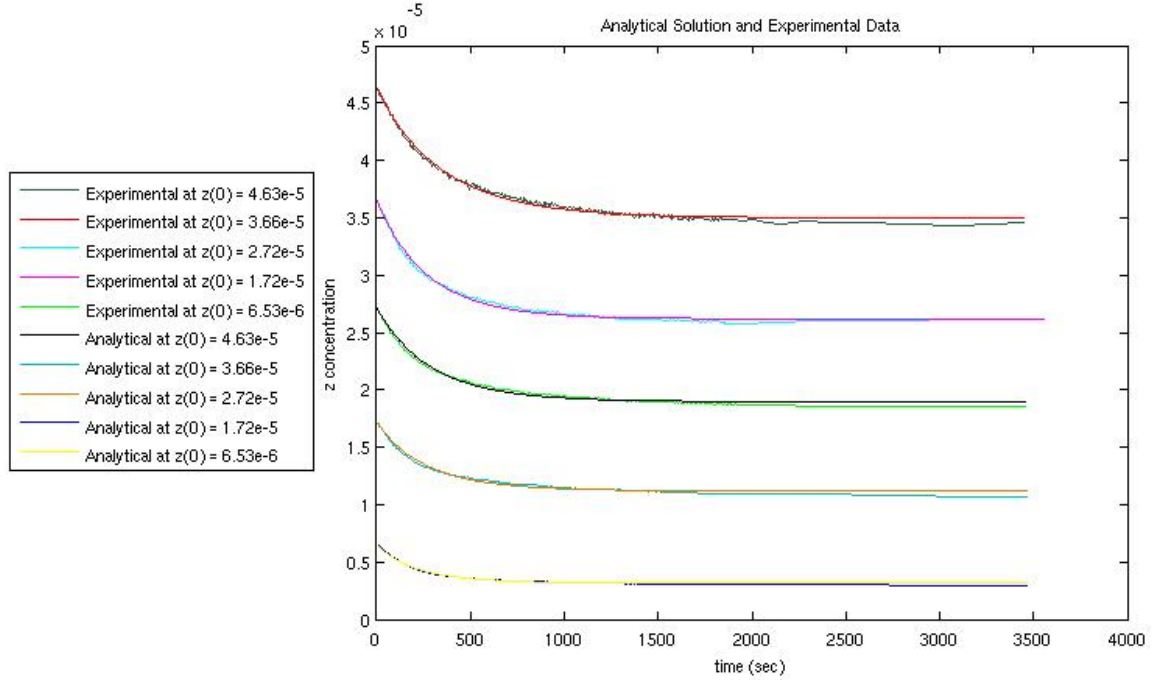
11

Figure 2: Analytical Solution with optimal rate constants obtained by least squares fitting compared with experimental data

As depicted by this figure, the analytical solution gives a reasonably good fit at the values for $k_2$ and $k_3$ from Table 1 above.

Another technique to test the validity of our analytical solution was to compute the value of $k_2$ using equation (26) by using the value of $k_3$ obtained numerically, the initial values for x, y, and z, and the data provided by Carnegie Mellon. Results are shown in Table 2, below.

| $z(0)$ | $4.63 \times 10^{-5}$ | $3.66 \times 10^{-5}$ | $2.72 \times 10^{-5}$ | $1.72 \times 10^{-5}$ | $6.53 \times 10^{-6}$ |
|---|---|---|---|---|---|
| $k_2$ | $3.3459 \times 10^3$ | $5.5875 \times 10^3$ | $5.6155 \times 10^3$ | $6.8480 \times 10^3$ | $1.1935 \times 10^4$ |

Table 2: Values of $k_2$ obtained through the analytical solution

12

These values for $k_2$ differ slightly from the values obtained doing the least squares fitting, shown in Figure 1 above. However, because there is not a large variation between the $k_2$ values obtained analytically and the $k_2$ values obtained numerically, this conveys that our analytical solution for z fits the data fairly well.

Lastly, another least squares fitting was done with a constraint minimization to ensure that all the rate values are nonnegative. The following table displays these results.

| $z(0)$ | $4.63 \times 10^{-5}$ | $3.66 \times 10^{-5}$ | $2.72 \times 10^{-5}$ | $1.72 \times 10^{-5}$ | $6.53 \times 10^{-6}$ |
|---|---|---|---|---|---|
| $k_2$ | $3.5444 \times 10^3$ | $5.3492 \times 10^3$ | $5.8402 \times 10^3$ | $7.2222 \times 10^3$ | $1.1404 \times 10^4$ |
| $k_3$ | $2.8620 \times 10^{-3}$ | $3.5023 \times 10^{-3}$ | $3.7374 \times 10^{-3}$ | $3.8239 \times 10^{-3}$ | $3.3971 \times 10^{-3}$ |

Table 3: Optimal values of $k_2$ and $k_3$ from least squares fitting with constraint minimization that all k values are positive

These rate constant values do differ, some more than others, from the values displayed in Table 1; plugging these values into the analytical solution show that some fit the data well and some curves diverge from the experimental data as time is increased. Figure 3, below, depicts these results.

For each of the $k_2$ and $k_3$ values that were found, there is a deviation between the $k_2$ values as well as a deviation between the $k_3$ values. Because $k_2$ and $k_3$ are known as constant reaction rates, one goal was to find the set of rate constants that fit all experimental data for all initial values of z. Our reaction rate values varied in order to fit each set of experimental data; one reason for this variation could be some error in experimentation. All experiments have some random error, which occurs because no measurement can be made with infinite precision. Another contributing factor could be the assumptions we made to
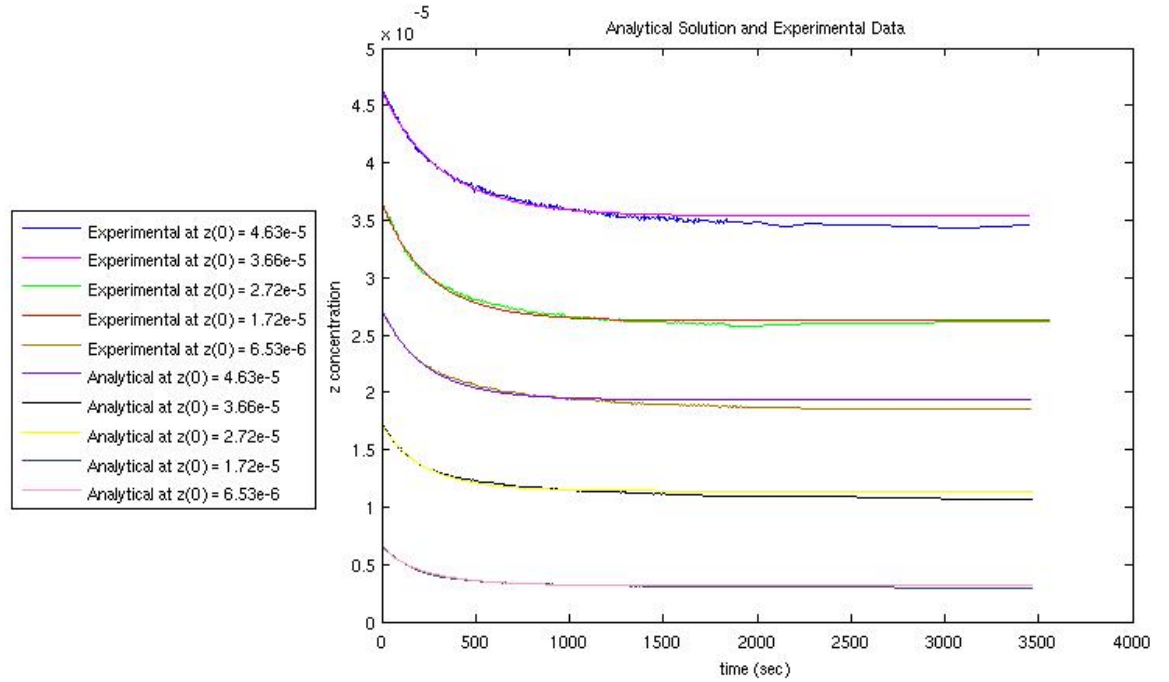
13

Figure 3: Analytical solution with optimal rate constant values obtained from least squares fitting with constraint minimization compared with experimental data

get the analytical solution. Our lienard system was originally a 2D nonlinear system, but we had reduced it to a linear system by assuming that $k_2$ was large, given some numerical results. It is possible that this nonlinearity in the lienard system is important and can alter and stabilize the values of $k_2$ and $k_3$. Lastly, the set of differential equations given by (1), (2), and (3) may not describe the system fully, and might have to be modified to produce comparable values for $k_2$ and $k_3$ at all initial conditions.

14

# 5    Conclusions and Future Work

For this project, numerical and analytical techniques were used to investigate the system of equations modeled by (1), (2), and (3). A least squares fitting was used to find values for $k_2$ and $k_3$ that minimized the error between the numerical curve and the experimental data. These rate constants were used to investigate how the analytical solution that was found fit the experimental data. For different data sets, different rate constants were found; for each set of rate constant values, the analytical solution did a fairly good job of matching the experimental data.

Because one set of rate constants should fit the experimental data for all initial values, more work can be done with this system. The chemists at Carnegie Mellon speculate that adding more terms to the system can yield more favorable results. The following set of differential equations will be investigated next.

$$\frac{dx}{dt} = -k_1^* x + k_2 yz - k_5 xy \tag{27}$$

$$\frac{dy}{dt} = k_1^* x - k_2 yz - k_3 y - k_4 y^2 - k_5 xy \tag{28}$$

$$\frac{dz}{dt} = -k_2 yz \tag{29}$$

For this system, the same numerical and analytical techniques will be used to find values for $k_2$ and $k_3$ and see how these values match the experimental data; an analytical solution will hopefully be obtained as well, and will also be used with the proper k values to determine how well it fits the data. Our previous analytical solution fit the data fairly well, but diverged in some places and could be improved upon; implementing these changes to this system might provide a better analytical solution that describes this system fully.

The phase space behavior of this system can also be explored using AUTO. As previously mentioned, the critical points and stability of the system were found. AUTO can be used to generate graphs that visually depict the behavior of the system at the critical points. Understanding the phase space behavior can also help chemists to predict how the system behaves from a chemical perspective.

# 6    References

[1] Platt, D. *Terry Collins Develops Green Catalysts for Potential Use in Industry and Biological Warfare. http : //www.cmu.edu/cmnews/saferliving.html.*

[2] Chanda, A., Ryabov, A.D, Mondal, S., et al. *Activity-Stability Parameterization of Homogenous Green Oxidation Catalysts.* Chemistry European Journal. 2006. Vol. 12, 9336-9345.

[3] Albarakati, W.A, Lloyd, N.G., Pearson, J.M. *Transformation to Lienard form.* Electronic Journal of Differential Equations. 2000. Vol 2000, No. 76, 1-11.